Green Synthesised Zinc Oxide Nanoparticles from Ulva Fasciata Algae Extract for Antibacterial and Supercapacitor Application

R.Balasubramanian[*1], S.Ravi [2]

[1*]*Research Scholar, Department of Physics, Annamalai University, Annamalai Nagar - 608 002, India,* bsubramanian379@gmail.com https://orcid.org/0009-0001-0788-5724

[2]*Associate Professor, Department of Physics (FEAT), Annamalai University, Annamalai Nagar - 608 002, India,* ambedravi1975@gmail.com https://orcid.org/0000-0002-2475

Abstracts: The present study aims to identify the green synthesized zinc oxide (ZnO) nanoparticles (NPs) from Ulva fasciata algae extract. The prepared ZnO NPs are characterized through XRD, FTIR, UV-Vis spectroscopy, SEM, TEM, EDX, antibacterial activity and electrochemical analysis. The XRD spectrum exposes the hexagonal structure. The FTIR spectrum reveals the functional group of ZnO NPs. The optical analysis gives the band gap values of ZnO at different concentrations of ulva fasciata algae extract. The antibacterial activities were tested S. aureus and E. coli. The CV curve exhibit a high specific capacitance of 45 F/g, at the scan rate of 10 mV/S.

Keywords: Green Synthesized Zno, *Ulva Fasciata Algae Extrct,* Antibacterial Activity and Electrochemical Analysis.

1. INTRODUCTION

Nanomaterials have novel and enhanced properties when compared to bulk materials, and their impact can be felt in almost all areas of science. Nanomaterials have unique properties in terms of chemical, physical, and mechanical aspects, and they can be used for a wide range of applications [1-2]. Researchers have recently focused on the discovery of novel nanomaterials, the construction of new nanostructures, and the exploration of their applications [3]. nanomaterials are synthesized using a wide range of methods. Currently, there is a surge in interest and development in green chemistry approaches for the synthesis of nanoparticles [5]. The environmentally friendly method of synthesis of nanomaterials using microorganisms, plant parts (tissue, fruit), and marine algae is appealing, and they are primarily used for cosmetic, water remediation, and medical applications [6]. In comparison to other physical and chemical methods of preparation, this method is a simple and cost-effective alternative. Ulva is a member of the Chlorophyta genus, a group of seaweeds grown in coastal areas. In general, the Ulva cell wall is divided into two polysaccharide groups. The main group is made up of soluble ulvan and insoluble cellulose, while the minor group is made up of linear alkali-soluble xyloglucan and glucuronan. Ulvan has distinct physiochemical and biological properties that illustrate its huge potential in a variety of applications, including food/feed, pharmaceutical, flavour, aquaculture, and agriculture industries etc.

Bacterial infectious diseases pose a significant economic and social risk to humanity. Because of the increasing emergence of new infectious diseases and the development of pathogenic bacterial resistance to existing drugs, it is critical to find new alternatives. Antibacterial materials seem to be important in a variety of industries, including the environment, food, packaging, healthcare, textile, and construction and decoration. When compared to organic antibacterial materials, inorganic antibacterial materials are more stable at high temperatures and harsh conditions. Metal oxide nanoparticles (CdO, ZnO, Mno2 and etc) are important antibacterial inorganic materials. These oxides are stable under extreme conditions and are generally considered safe for animals and humans [7-9]. Among them Zinc oxide nanomaterials is really a significant area of research due to their unique properties and wide range of applications. In this, we prepared ZnO NPs by using Ulva fasciata algal extract.

2. EXPERIMENTAL PROCEDURE

2.1 Ulva Fasciata Extract Preparation

For this preparation, Ulva fasciata algae were collected from Rameswaram costal area (Tamil nadu, India). And the collected Ulva fasciata algae were washed with DI water until it reaches the value of pH 7. Then washed Ulva fasciata algae was dried oven at 60˚C for 12 hrs. After that, the dried Ulva fasciata algae were grinded by using agate mortar. For the extract preparation, 10g of dried ulva fasciata algae is dissolved in 100 ml of DI water and stirred continuously for 1hr. after that homogeneous solution is heated at 100˚C for 15 min. then extract is filtered with whatman No. 1 filter paper. The filtered ulva fasciata algae extract is used for ZnO NPs.

2.2 Preparation of ZnO Nannoparticles

0.1 M of Zinc nitrate hexahydrate is dissolved in 20 ml solvent of ulva fasciata algae extract and stirred continuously for an hour. After that the homogeneous product was dried at 100˚C for 4 hrs. Then the dried product was collected and calcinated at 400˚C for 2 hrs. The same procedure is repeated for 30 ml and 40 ml of ulva fasciata extract.

2.3 Electrode Preparation

The working electrode (ZnO) is prepared by the following method. 80:10:10 ratio of ZnO, PVDF and carbon black was taken and grind it smoothly, after that NMP solution was added with the well grind composite. The composite was grind until it reaches slurry form. The prepared slurry was coated on (1X1) cm nickel plate evenly. Then the coted plate was dried in oven at 100˚C for 6 hrs. The working electrode was analyzed by Biologic – SP 300 instrument. 1M KOH was used as an electrolyte solution.

3. RESULT AND DISCUSSION

3.1 XRD Analysis

Fig. 1 (a, b and c) represents the XRD spectrum of prepared Zno NPs at three different concentration of ulva fasciata algae extract (20 ml, 30 ml and 40 ml). The XRD peaks observed at 31°, 34°, 36°, 47°, 56°, 62°, 66°, 67° and 69° are related to the planes at (100), (002), (101), (102), (110), (103), (200), (112) and (201) respectively. The observed planes clearly evident that the synthesized ZnO is formed with hexagonal crystal structure according to JCPDS Card No. 89-1397 [9-11]. Also, the XRD peaks indicate that the Zno sample synthesized at 20 ml is not well formed. As ulva fasciata algae extract concentration increases to 40 ml, the XRD peaks appeared as sharp with high intensity indicating that the prepared Zno at 40 ml is highly crystalline nature and without any impurities compared to ZnO at 20 ml and ZnO at 30 ml. The d spacing value of the intense XRD peak appeared at $2\theta = 36°$ is 0.25 nm.

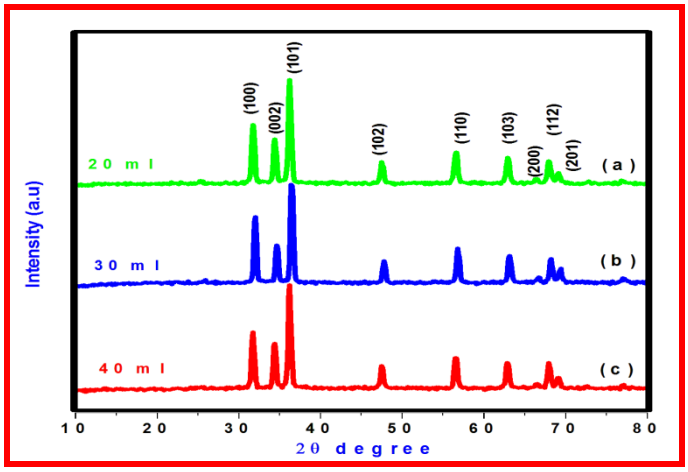

Figure 1: XRD pattern of ZnO NPs (a) 20 ml of ulva fasciata extract, (b) 30 ml of ulva fasciata extract and (c) 40 ml of ulva fasciata extract

The different structural parameters of the ZnO NPs are evaluated using the following equations.

Crystallite size $D=K\lambda/(\beta \cos\theta) = 0.9\lambda/(\beta \cos\theta)$ … (1)

Where 'λ' is the Wavelength, 'β' is the Full-width half maximum and 'θ' is Bragg's angle.

Microstrain $= \beta\cos\theta/4$ … (2)

Dislocation density $\delta = 1/D^2$ … (3)

Where n is equal to unity and D is the crystalline size.

Lattice parameters $1/(d_{hkl}^2) = h^2/a^2 + k^2/b^2 + l^2/c^2$ … (4)

where, 'dhkl' represents the interplanar spacing and 'hkl' is the Miller indices. The calculated structural parameters of the synthesized ZnO NPs by using ulva fasciata algae extract (20 ml, 30 ml and 40 ml) are listed in the table 1.

Table 1: structural parameters of ZnO nanoparticles

S.No.	Extract (ml)	Crystal size (nm)	Dislocation density (δ) 10^{15} (lines/m^2)	Microstrain X 10^{-3}	Lattice parameters	
					a=b	c
1	20	21	55.21	1.33	3.53	5.30
2	30	18	58.16	1.55	3.58	5.34
3	40	16	64.34	1.78	3.63	5.38

From table 1, it is noted that the crystallite size increases with ulva fasciata algae extract concentration, whereas the microstrain and dislocation density decreases which indicates lesser imperfection in the crystal lattice.

3.2 FTIR Analysis

FTIR measurement was performed to study the vibrational properties and functional group analysis of ZnO nanoparticles. The analysis is carried out from 400 cm-1 to 4000 cm-1. From the Fig. 2, the IR bands noted in the ZnO spectrum are 450 cm-1, 1111 cm-1, 1433 cm-1, 1625 cm-1, 2920 cm-1 and 3389 cm-1 [13-15]. The bands observed at 3421 cm-1 and 1625 cm-1 correspond to the O-H stretching and bending vibrational modes of water molecules. The band observed at 1111 cm-1 is related to the symmetric stretching vibration of C-C bond. The band observed at 2920 cm-1 is represents CH2 and it attributed to the plant phenolics. The peak observed at 1433 cm-1 represents the C-OH stretching vibration. The characteristic peak ZnO appeared at 450 cm-1 which evidently confirms the formation of ZnO nanoparticles.

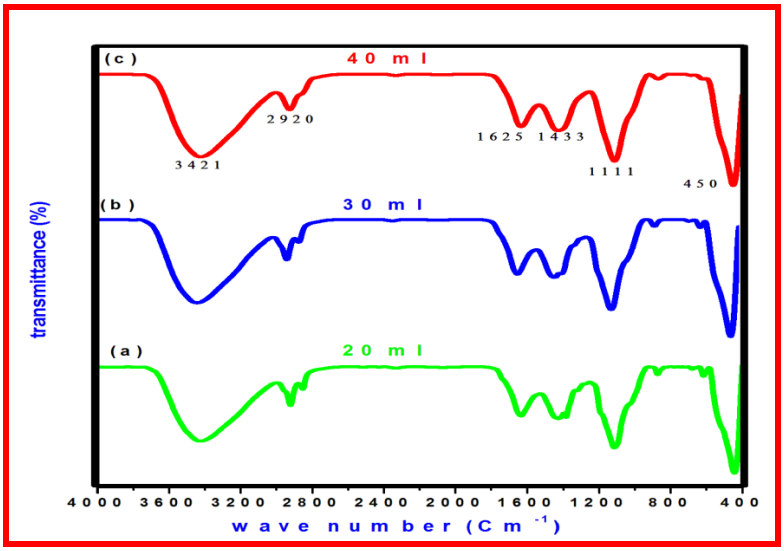

Figure 2: FTIR spectrum of ZnO NPs (a) 20 ml of ulva fasciata extract, (b) 30 ml of ulva fasciata extract and (c) 40 ml of ulva fasciata extract

3.3 UV- Vis Analysis

Fig 3 (a-c) shows the UV vis spectrum of green synthesized ZnO NPs. three absorption peaks are observed at 249 nm, 244 nm and 243 nm corresponds to 20 ml , 30 ml and 40 ml of ZnO NPs using Ulva fasciata algae extract respectively. These peaks are appear due to the collective oscillation of free conduction band electrons excited by incident electromagnetic radiation causing surface plasmon absorption in ZnO nanoparticles [13]. The tauc plot is used to identify the band gap energy of ZnO nanoparticles. Fig 4 (a-c) shows the tauc UV spectrum of ZnO nanoparticles prepared by 20 ml, 30 ml and 40 ml ulva fasciata leaf extract respectively.

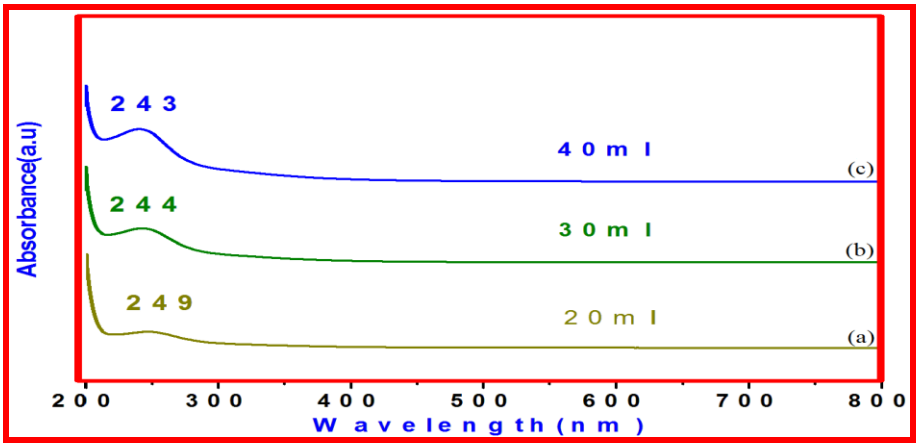

Figure 3: UV vis spectrum of ZnO NPs (a) 20 ml of ulva fasciata extract, (b) 30 ml of ulva fasciata extract and (c) 40 ml of ulva fasciata extract

The following tauc equation is used find out the band gap of ZnO nanoparticles.

Tauc's plot is used to calculate the energy band gap. You can find Tauc's equation using

$$\alpha h\nu = A(h\nu - E_g)^n \quad \ldots(5)$$

Where A is the constant, hv is the photon energy, is the absorption coefficient, and Eg is the energy bandgap. Depending on whether the transition from the valence band to the conduction band is direct or indirect, the value of n is either 1/2 or 2. If the transition is direct, the value is 1/2 and if it is indirect, it is 2. ZnO has a straight band structure, therefore n is equal to 1/2. The equation then has the following form.

$$(\alpha h\nu)1\backslash 2 = B(h\nu - E_g) \quad \ldots(6)$$

where B is a constant referring to the charge carriers' effective masses in relation to the valence and conduction bands.

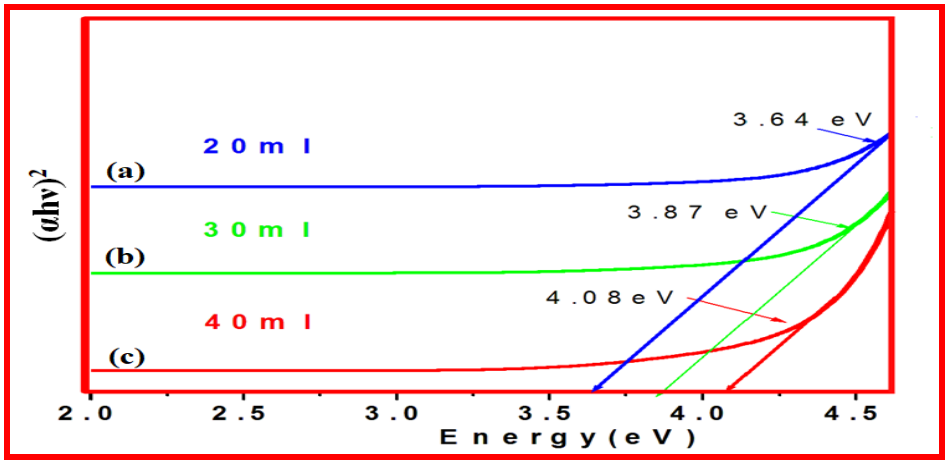

Figure 4: Tauc plot of ZnO NPs (a) 20 ml of ulva fasciata extract, (b) 30 ml of ulva fasciata extract and (c) 40 ml of ulva fasciata extract.

From the graph, the band gap values of 20 ml, 30 ml and 40ml ulva fasciata algae extract ZnO NPs and 3.64 eV, 3.87 eV and 4.08 eV respectively.

3.4 Microstructural and Elemental composition analysis of ZnO Nanoparticles

Fig. 5 (a - b) shows the SEM morphologies of the ZnO nanoparticles. From the Fig. 5a, it can be seen that the ZnO nanoparticles are formed as nanosheet. As can be seen from the Fig. 5 (b), the surface morphology of the ZnO nanoparticles becomes smoother with the nanosheets are widened and visible like nanosheet structure. This is due to the reason that Zn ions get incorporated into the O ions and the sheets get widened and forms nanosheet like structures [16].

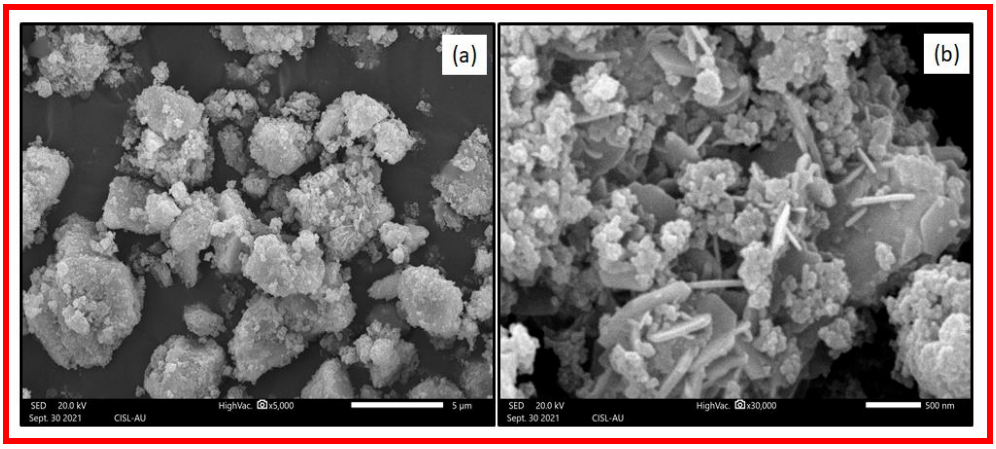

Figure 5: (a&b) SEM images of bio synthesized ZnO nanoparticles

The morphology, microstructure and crystallite nature of the ZnO nanoparticles were considered by TEM analysis with SAED pattern, respectively. TEM image ZnO NPs are shown in Fig. 6(a, b) and it is noticed that nanoparticles are shown in nanosheet morphology. Fig. 6(c) shows the high resolution TEM image of ZnO nanoparticles. The measured distance between the lattice fringes are 0.24 nm, analogous to the (101) plane of hexagonal crystal structure of ZnO NPs. In Fig. 6 (d), the SAED pattern of the ZnO nanoparticles show the well-defined diffraction ring pattern at (101) plane and this illustrates the polycrystalline structure.

The EDX spectra of ZnO nanoparticles were carried out to confirm the presence of Zn and O elements in the prepared nanoparticles. Fig. 7 shows the EDX spectra of ZnO nanoparticles with the mass percentages of 66.44% and 10.39% confirms the presence of Zn and O element respectively. Other minor elements appeared due to the chemical composition of Ulva fasciata algae extract. Table 2 shows the elemental composition of green synthesized ZnO nanoparticles.

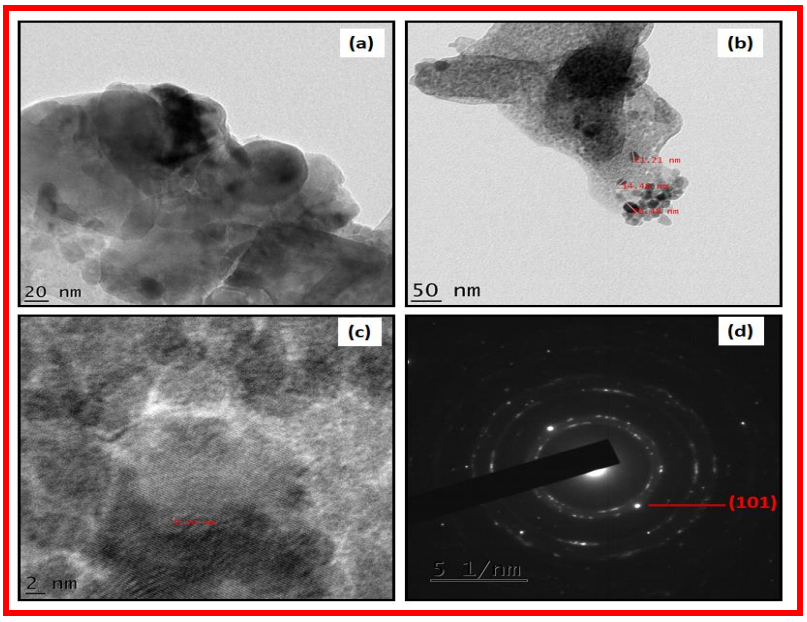

Figure 6: (a&b) HRTEM images of ZnO NPs. (c) d spacing fringes and (d) SAED pattern ZnO nanoparticles

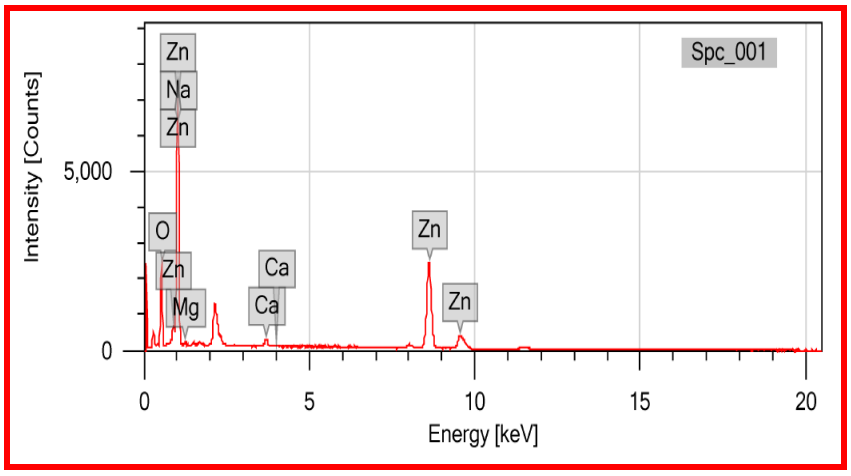

Figure 7: EDX spectrum of ZnO nanoparticles

Table 2: Elemental composition of ZnO nanoparticles

Element	Line	Mass%	Atom%
O	K	10.39±0.10	24.46±0.23
Na	K	21.54±0.22	35.29±0.36
Mg	K	0.70±0.05	1.08±0.08
Ca	K	0.93±0.04	0.88±0.03
Zn	K	66.44±0.46	38.29±0.27
Total		100.00	100.00
Spc_001			Fitting ratio 0.2025

3.5 Antibacterial activity of ZnO nanoparticles

The disc diffusion method was employed to evaluate the antibacterial activity of green synthesised ZnO NPs against one gram positive bacteria S. aureus and one gram negative bacteria E. coli. The antibacterial activity of green synthesised CuO NPs against (a) S. aureus and (b) E. coli at two different concentrations (50 µl and 100 µl) is shown in Fig. 8. The resultant parameters are shown in table 3. In each of the petri plates, the appearance of an inhibition zone around the wells clearly demonstrated the antibacterial potential of green synthesized ZnO NPs [17-19]. ZnO nanoparticles have antibacterial activity against both gram positive and gram negative test strains. CuO NPs had a strong antibacterial effect on gram negative bacteria E.coli [19-23]. The antibacterial activity mechanism is based on ZnO NPs penetrating the bacterial cell membrane, causing membrane damage and cell death. Owing their nanosize and high surface-to-volume ratio, ZnO NPs interacted with the bacterial membrane. ZnO NPs were found to have a greater inhibitory effect on gram negative bacteria than on gram positive bacteria in this study, which could be attributed to differences in bacterial membrane structures. As a result, ZnO NPs synthesised from uluva algae extract have been found to be an effective antibacterial agent against gram negative (E. coli) bacteria [24-27].o

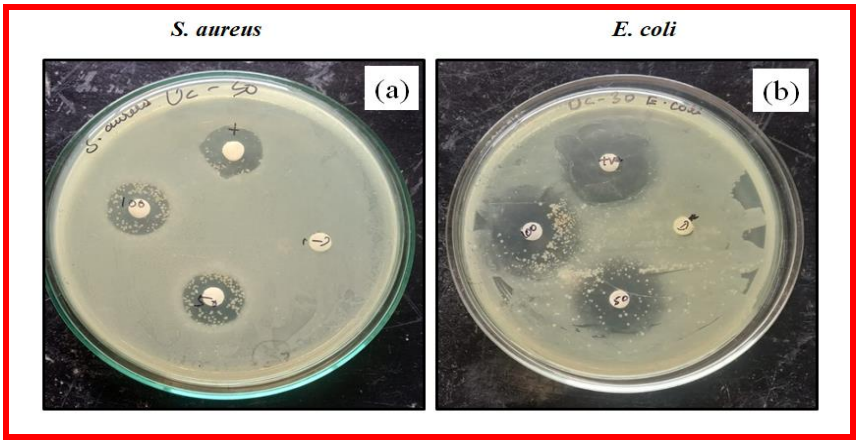

Figure 8. shows the antibacterial activity of green synthesized ZnO NPs against (a) S. aureus and (b) E. coli

Table 3: Antibacterial activity result of ZnO nanoparticles

Test bacterial pathogens	Zone of inhibition (mm)	
	50 µg	100 µg
S. aureus	6.08±0.48	8.10±0.28
E. coli	9.08±0.18	12.65±0.42

3.7 Electrochemical performance of ZnO Nanoparticles

The electrochemical performance of ZnO electrode was evaluated by CV and GCD curves. Fig. 9 shows the CV curves of ZnO electrode at the scan rates of 10 mV/s, 25 mV/s, 50 mV/s, 75 mV/s and 100 mV/s, respectively with the potential window of 0V to 0.6V. From figure, it could be observed that ZnO nanomaterial possess well-defined oxidation and redox peaks, which implies the ideal pseudocapacitive behavior of the prepared electrode.

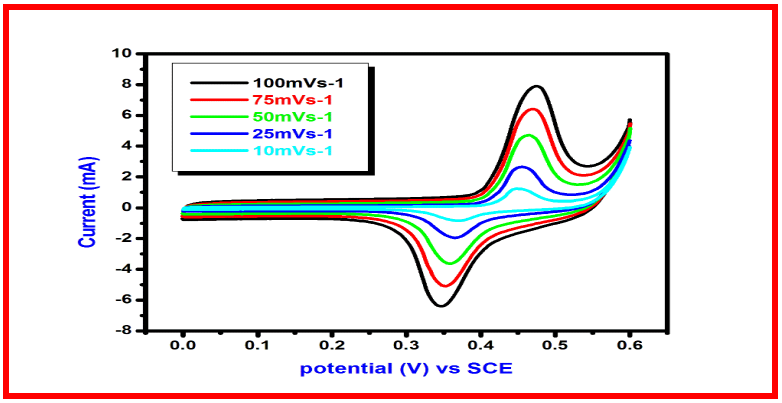

Figure 9: CV cure of ZnO nanoparticles

The specific capacitance ZnO electrodes can be calculated by using the equation

$$Cp = A/m\Delta V \quad \ldots (7)$$

Where Cp, A, m and ΔV represent the cathodic and anodic charge on each scan rate, the area under the CV curve, the mass of the active material (mg) and the scan rate in mV/s. The calculated values of specific capacitance are 45 F/g, 40 F/g, 36 F/g, 33 F/g and 32 F/g for ZnO electrode at the scan rate of 10 mV/s, 25 mV/s, 50 mV/s, 75 mV/s and 100 mV/s, respectively. At the lower scan rate the specific capacitance of ZnO exhibit high, which indicates the electrolytic ions are more interact with inner and outer layer of electrode[14-16]. At higher scan rate the ionic interaction arise only the outer layer of electrode so it exhibits low specific capacitance.The supercapacitor performance of the ZnO electrode was further examined by GCD curves. Fig. 10 shows GCDs curves of ZnO electrode. From the GCDs curves, it is observed that the discharging time of 1 A/g (current density) increases compared to 2 A/g (current density). The specific capacitance of ZnO electrodes is calculated from GCD curves using the equation 8.

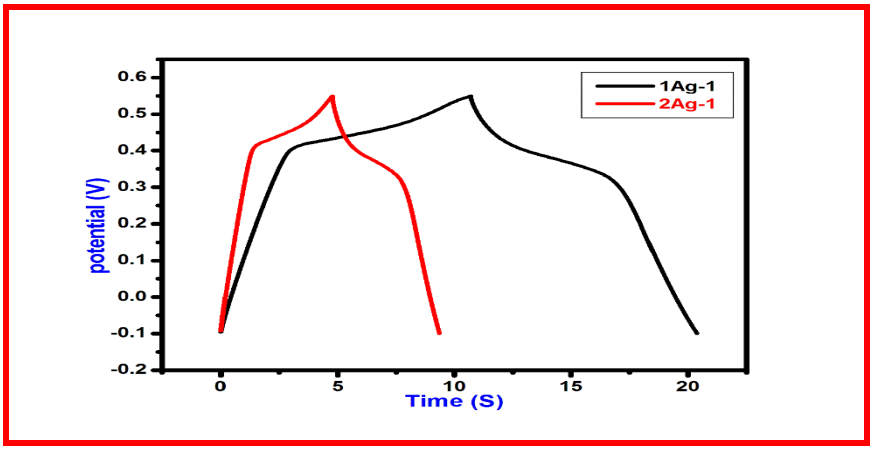

Figure 10: GCD cure of ZnO nanoparticles

The Cp of ZnO electrodes using GCDs can be calculated from the following equation

$$Cp\ (GCD) = i\Delta t/m\Delta V \quad \ldots (8)$$

Where i is the current density (A/g), Δt is the discharging time (s), m is the mass of the active material (mg) and ΔV is the potential window (volts). The calculated Cp values of ZnO electrode are 16 F/g and 15F/g for current density of 1 A/g and 2 A/g respectively. As the current density increases, the specific capacitance decreases due to increase in ohmic drop during the charge/discharge process [17-18].

CONCLUSION

The green synthesized ZnO NPs were prepared by using Ulva fasciata algae extract. The XRD spectrum confirms the hexagonel structure of ZnO nanoparticles and the diffraction planes are very well coincide with JCPDS card number 89-1397. The FTIR spectrum confirms the functional group present in ZnO NPs. The band gap values of ZnO NPs is increased when the crystallite size of the NPs are decreased. The green synthesized CuO NPs was act effective antibacterial agent against gram negative (E. coli) bacteria. From the electrochemical analysis result, the ZnO NPs is highly suitable for supercapacitor application.

REFERENCES

[1]. Madany, M. A., Abdel-Kareem, M. S., Al-Oufy, A. K., Haroun, M., & Sheweita, S. A. (2021). The biopolymer ulvan from Ulva fasciata: Extraction towards nanofibers fabrication. International Journal of Biological Macromolecules, 177, 401-412.

[2]. Chakraborty, K., & Paulraj, R. (2010). Sesquiterpenoids with free-radical-scavenging properties from marine macroalga Ulva fasciata Delile. Food Chemistry, 122(1), 31-41.

[3]. Vishnupriya, B., Nandhini, G. E., & Anbarasi, G. (2022). Biosynthesis of zinc oxide nanoparticles using Hylocereus undatus fruit peel extract against clinical pathogens. Materials Today: Proceedings, 48, 164-168.

[4]. Agarwal, H., Nakara, A., Menon, S., & Shanmugam, V. (2019). Eco-friendly synthesis of zinc oxide nanoparticles using Cinnamomum Tamala leaf extract and its promising effect towards the antibacterial activity. Journal of Drug Delivery Science and Technology, 53, 101212.

[5]. Mirza, A. U., Kareem, A., Nami, S. A., Bhat, S. A., Mohammad, A., & Nishat, N. (2019). Malus pumila and Juglen regia plant species mediated zinc oxide nanoparticles: Synthesis, spectral characterization, antioxidant and antibacterial studies. Microbial pathogenesis, 129, 233-241.

[6]. Soren, S., Kumar, S., Mishra, S., Jena, P. K., Verma, S. K., & Parhi, P. (2018). Evaluation of antibacterial and antioxidant potential of the zinc oxide nanoparticles synthesized by aqueous and polyol method. Microbial pathogenesis, 119, 145-151.

[7]. Yadav, S., Rani, N., & Saini, K. (2022). Green synthesis of ZnO and CuO NPs using Ficus benghalensis leaf extract and their comparative study for electrode materials for high performance supercapacitor application. Materials Today: Proceedings, 49, 2124-2130.

[8]. Lianga, S. X. T., Wong, L. S., Lim, Y. M., Djearamanea, S., & Lee, P. F. (2020). Effects of Zinc Oxide nanoparticles on Streptococcus pyogenes. South African Journal of Chemical Engineering, 34(1), 63-71.

[9]. Esparza-González, S. C., Sánchez-Valdés, S., Ramírez-Barrón, S. N., Loera-Arias, M. J., Bernal, J., Meléndez-Ortiz, H. I., & Betancourt-

Galindo, R. (2016). Effects of different surface modifying agents on the cytotoxic and antimicrobial properties of ZnO nanoparticles. Toxicology in Vitro, 37, 134-141.

[10]. Rajivgandhi, G. N., Ramachandran, G., Maruthupandy, M., Manoharan, N., Alharbi, N. S., Kadaikunnan, S.& Li, W. J. (2020). Anti-oxidant, anti-bacterial and anti-biofilm activity of biosynthesized silver nanoparticles using Gracilaria corticata against biofilm producing K. pneumoniae. Colloids and Surfaces A: Physicochemical and Engineering Aspects, 600, 124830.

[11]. Dhanemozhi, A. C., Rajeswari, V., & Sathyajothi, S. (2017). Green synthesis of zinc oxide nanoparticle using green tea leaf extract for supercapacitor application. Materials Today: Proceedings, 4(2), 660-667.

[12]. Danial, E. N., Hjiri, M., Abdel-Wahab, M. S., Alonizan, N. H., El Mir, L., & Aida, M. S. (2020). Antibacterial activity of In-doped ZnO nanoparticles. Inorganic Chemistry Communications, 122, 108281.

[13]. Pandimurugan, R., & Thambidurai, S. (2017). UV protection and antibacterial properties of seaweed capped ZnO nanoparticles coated cotton fabrics. International journal of biological macromolecules, 105, 788-795.

[14]. Fang, L., Zhang, B., Li, W., Zhang, J., Huang, K., & Zhang, Q. (2014). Fabrication of highly dispersed ZnO nanoparticles embedded in graphene nanosheets for high performance supercapacitors. Electrochimica Acta, 148, 164-169.

[15]. Kumar, A. (2020). Sol gel synthesis of zinc oxide nanoparticles and their application as nano-composite electrode material for supercapacitor. Journal of Molecular Structure, 1220, 128654.

[16]. Samuel, E., Londhe, P. U., Joshi, B., Kim, M. W., Kim, K., Swihart, M. T. & Yoon, S. S. (2018). Electrosprayed graphene decorated with ZnO nanoparticles for supercapacitors. Journal of Alloys and Compounds, 741, 781-791.

[17]. Chee, W. K., Lim, H. N., Harrison, I., Chong, K. F., Zainal, Z., Ng, C. H., & Huang, N. M. (2015). Performance of flexible and binderless polypyrrole/graphene oxide/zinc oxide supercapacitor electrode in a symmetrical two-electrode configuration. Electrochimica Acta, 157, 88-94.

[18]. Anand, G. T., Renuka, D., Ramesh, R., Anandaraj, L., Sundaram, S. J., Ramalingam, G., ... & Kaviyarasu, K. (2019). Green synthesis of ZnO nanoparticle using Prunus dulcis (Almond Gum) for antimicrobial and supercapacitor applications. Surfaces and Interfaces, 17, 100376.

[19]. Vijayakumar, S., Krishnakumar, C., Arulmozhi, P., Mahadevan, S., & Parameswari, N. (2018). Biosynthesis, characterization and antimicrobial activities of zinc oxide nanoparticles from leaf extract of Glycosmis pentaphylla (Retz.) DC. Microbial pathogenesis, 116, 44-48.

[20]. Nair, M. G., Nirmala, M., Rekha, K., & Anukaliani, A. (2011). Structural, optical, photo catalytic and antibacterial activity of ZnO and Co doped ZnO nanoparticles. Materials letters, 65(12), 1797-1800.

[21]. Ishwarya, R., Vaseeharan, B., Subbaiah, S., Nazar, A. K., Govindarajan, M., Alharbi, N. S., ... & Al-Anbr, M. N. (2018). Sargassum wightii-synthesized ZnO nanoparticles–from antibacterial and insecticidal activity to immunostimulatory effects on the green tiger shrimp Penaeus semisulcatus. Journal of Photochemistry and Photobiology B: Biology, 183, 318-330.

[22]. El-Belely, E. F., Farag, M. M., Said, H. A., Amin, A. S., Azab, E., Gobouri, A. A., & Fouda, A. (2021). Green synthesis of zinc oxide nanoparticles (ZnO-NPs) using Arthrospira platensis (Class: Cyanophyceae) and evaluation of their biomedical activities. Nanomaterials, 11(1), 95.

DOI: https://doi.org/10.15379/ijmst.v10i3.3024